LETTERS

# An excitable gene regulatory circuit induces transient cellular differentiation

Gürol M. Süel[1], Jordi Garcia-Ojalvo[2], Louisa M. Liberman[1] & Michael B. Elowitz[1]

**Certain types of cellular differentiation are probabilistic and transient[1–3]. In such systems individual cells can switch to an alternative state and, after some time, switch back again. In *Bacillus subtilis,* competence is an example of such a transiently differentiated state associated with the capability for DNA uptake from the environment. Individual genes and proteins underlying differentiation into the competent state have been identified[4,5], but it has been unclear how these genes interact dynamically in individual cells to control both spontaneous entry into competence and return to vegetative growth. Here we show that this behaviour can be understood in terms of excitability in the underlying genetic circuit. Using quantitative fluorescence time-lapse microscopy, we directly observed the activities of multiple circuit components simultaneously in individual cells, and analysed the resulting data in terms of a mathematical model. We find that an excitable core module containing positive and negative feedback loops can explain both entry into, and exit from, the competent state. We further tested this model by analysing initiation in sister cells, and by re-engineering the gene circuit to specifically block exit. Excitable dynamics driven by noise naturally generate stochastic and transient responses[6], thereby providing an ideal mechanism for competence regulation.**

Upon encountering nutrient limitation, a minority of *B. subtilis* cells become competent for DNA uptake while most commit irreversibly to sporulation (Fig. 1a). Extensive research has elucidated a detailed map of molecular interactions that comprise the *B. subtilis* competence control circuit (Supplementary Fig. S1)[4,5]. At the heart of this circuit is the ComK 'master' transcription factor (Fig. 1b). ComK activates expression of a suite of genes necessary for competence, including the *comG* operon (Fig. 1b)[7–10]. ComK also activates its own expression, and two recent studies have shown that this positive feedback loop is critical for the induction of competence[11,12]. Upon entry into stationary phase, *comK* is expressed at a basal level, but is also rapidly degraded by the MecA complex, a multiprotein assembly that includes the ClpP–ClpC proteases[13]. Independent studies have shown that the ComS peptide competitively inhibits ComK degradation by the MecA complex[13,14]. Expression of ComS thus favours induction of competence by allowing ComK levels to build up sufficiently to enable full ComK activation by positive autoregulation. Despite the important role of ComS in inducing competence, its expression is activated by stress and cell–cell signalling and is therefore high in all cells under stress, not just those destined to become competent[7]. Interestingly, overexpression of ComK was suggested to suppress expression of *comS*[7]. This implies the existence of an indirect negative feedback loop acting upon ComK, which might affect exit from competence (Fig. 1b). Therefore, we consider here interactions among the MecA complex, *comK* and *comS*, which we collectively refer to as the 'MeKS' module.

Differentiation into the competent state is difficult to study by traditional methods that average over large populations: the process affects a small minority of cells in a non-synchronous manner. Here we built strains in which activities of different pairs of promoters within the circuit could be monitored simultaneously in the same cell, revealing interactions between circuit components that could not be obtained by observing the same genes one at a time. Pairwise combinations of the promoters $P_{comG}$, $P_{comK}$ and $P_{comS}$ expressing *yfp* or *cfp* were inserted into standard sites within the *B. subtilis* chromosome, leaving the endogenous genes intact (see Supplementary Information). We analysed these strains using automated time-lapse fluorescence microscopy, and quantitative image analysis[15], under conditions where the overall frequency of competence events was $3.6 \pm 0.7\%$ (26 out of 725 cell division events generated competent cells).

The resulting data can be interpreted in terms of a mathematical model of the MeKS module. As described in Box 1, the MeKS model is a dynamical system that exhibits excitability: relatively small, threshold-crossing perturbations trigger large-amplitude excursions in phase space that eventually return the system to its initial state[6]. Correspondingly, in the cell, stochastic effects in gene expression have been shown to generate significant variability[16,17]. Such biochemical 'noise' can initiate a sequence of intracellular events—changes in gene expression and protein degradation—that cause cells to transiently differentiate into the competent state and subsequently return to vegetative growth. Noise-driven excitable systems naturally exhibit the two key characteristics of competence: probabilistic and transient activation.

To explore these properties further, we first simultaneously measured $P_{comG}$ and $P_{comK}$ promoter activities in single competent cells. $P_{comG}$ and $P_{comK}$ are both regulated by ComK, but $P_{comK}$ also has many other important transcriptional inputs (Supplementary Fig. S1). This experiment evaluates the significance of these other transcriptional inputs into $P_{comK}$ during competence. Figure 2a shows frames from recorded film footage of a *B. subtilis* microcolony under nutrient limitation conditions, in which most cells eventually sporulate (see also Supplementary Movie 1). In this example, a single cell within the microcolony becomes competent and consequently its cell division is blocked, as previously reported[18]. As $P_{comG}$ and $P_{comK}$ activities decline during exit from competence, the elongated cell undergoes multiple septation events and returns to the vegetative state. Quantitative time traces of the fluorescence levels show strong correlation between $P_{comG}$ and $P_{comK}$ in this film footage (Fig. 2b). This behaviour is representative of all measured events in this strain ($n = 37$) (Fig. 2c). The high degree of correlation between $P_{comG}$ and $P_{comK}$ suggests that other transcriptional inputs to the ComK promoter do not significantly affect ComK expression during competence.

In the MeKS model, ComK indirectly represses ComS, generating an anti-correlation between $P_{comG}$ and $P_{comS}$ activities. The regulation

[1]Division of Biology and Department of Applied Physics, California Institute of Technology, Pasadena, California 91125, USA. [2]Departament de Física i Enginyeria Nuclear, Universitat Politècnica de Catalunya, Colom 11, E-08222 Terrassa, Spain.

of *comS* is, however, known to be complex, having several transcriptional inputs (Supplementary Fig. S1)[19–21]. To test the prediction of the MeKS model we constructed a strain containing copies of the $P_{comG}$ and $P_{comS}$ promoters expressing *cfp* and *yfp*, respectively. As shown in Fig. 3a and Supplementary Movie 2, all cells express $P_{comS}$ to varying degrees. In cells that become competent, $P_{comG}$ activity increases as $P_{comS}$ activity decreases. Later, as $P_{comG}$ activity shuts off and septation begins, $P_{comS}$ activity increases again. This striking negative correlation between $P_{comG}$ and $P_{comS}$ activities is present during both entry and exit from competence, although it is more closely synchronized during entry (Fig. 3b). This behaviour is representative of data obtained from all competent cells of the same strain ($n = 31$) (Fig. 3c), and is consistent with negative regulation of *comS* by ComK. Furthermore, the negative correlation is specific to competence, as is evident from the behaviour of the non-competent sister cell in Fig. 3b.

A fundamental question is whether initiation of competence is stochastic or affected by memory of previous events. Escape from competence returns promoter activities to pre-competence levels, suggesting the possibility of successive episodes of competence. Indeed, as shown in Fig. 3d, two consecutive competence events can be observed in a single cell lineage, showing that cells retain the potential to re-initiate competence. In fact, re-initiation occurred with a frequency of 6.0 ± 2.0% ($n = 9$ events out of 151), not significantly different from the overall competence frequency (3.6 ± 0.7%). Repeated competence events are neither favoured nor suppressed. This evidence for stochastic initiation of competence is further supported by analysis of competence events in sister cell pairs (Supplementary Information). Cells were not significantly more or less likely to become competent if their sister became competent (conditional frequency = 4.1 ± 0.9%, $n = 19$ events out of 463). When two sisters do become competent together, the amount of time one spends in competence is uncorrelated with that of its sister cell (Kolmogorov–Smirnov test; $n = 36$). These results are consistent with a stochastic and memory-less model for competence initiation and duration.

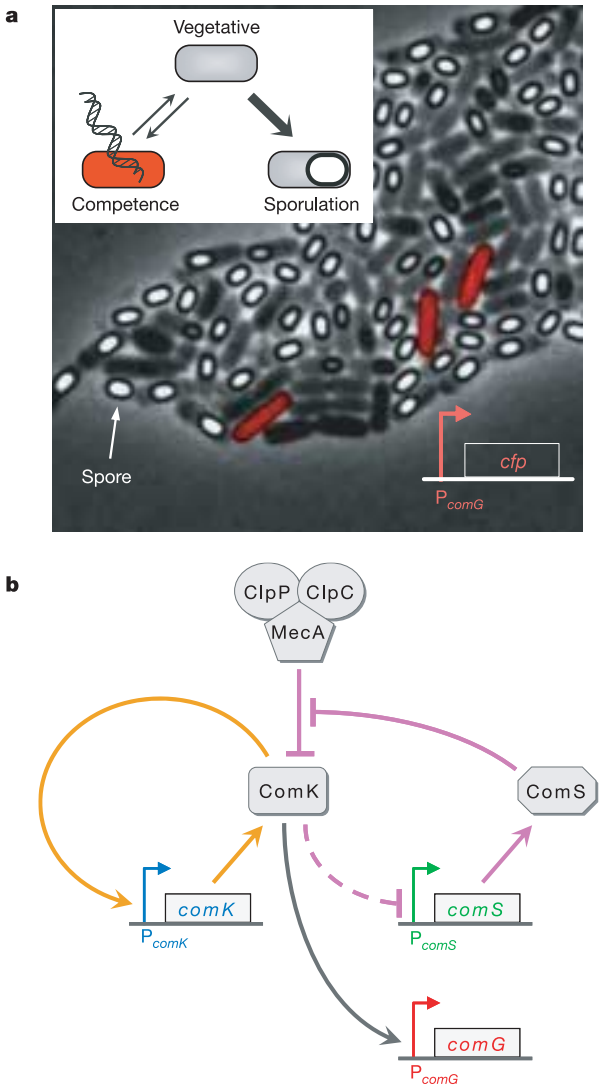


**Figure 1 | Stress response in *B. subtilis* and the core competence circuit.** **a**, Snapshot of a *B. subtilis* microcolony in nutrient-limited conditions. *cfp* expression from $P_{comG}$ is shown in red. Inset: a flow chart illustrating developmental paths connecting the vegetative, spore forming and competent states. **b**, Map of interactions within the core competence circuit (MeKS). The transcriptional autoregulatory positive feedback loop of ComK and the ComS-mediated indirect negative feedback loop are depicted in orange and purple, respectively. ComS competes with ComK for degradation by the MecA–ClpP–ClpC complex, effectively interfering with degradation of ComK (curved purple inhibitory arrow). The dashed purple line from ComK to $P_{comS}$ denotes indirect repression. The activities of the promoters labelled in red, blue and green were measured in this study. These colours are used to represent the corresponding promoters throughout the figures.

**Box 1 | The dynamical model of competence induction**

To understand how the MeKS network structure determines the dynamics of competence, we built a mathematical model constrained by experimental observations (see Supplementary Information). This model can be reduced to a system of two stochastic ordinary differential equations incorporating both the direct positive and the ComS-mediated negative feedback loops of ComK. In dimensionless form:

$$\frac{dK}{dt} = a_k + \frac{b_k K^n}{k_0^n + K^n} - \frac{K}{1+K+S} \quad (1)$$

$$\frac{dS}{dt} = \frac{b_s}{1+(K/k_1)^p} - \frac{S}{1+K+S} + \xi(t) \quad (2)$$

Here, $K$ and $S$ represent the concentration levels of ComK and ComS protein, respectively. $a_k$ and $b_k$ represent minimal and fully activated rates of ComK production, respectively. $k_0$ is the concentration of ComK required for 50% activation. The cooperativities of ComK auto-activation and ComS repression are parameterized by the Hill coefficients $n$ and $p$, respectively. Expression of ComS has maximum rate $b_s$ and is half-maximal when $K = k_1$. Enzymatic MecA-mediated degradation affects both ComK and ComS; the form of the corresponding nonlinear degradation terms expresses a competitive mechanism, which is the only source of coupling from ComS to ComK. Random fluctuations in ComS expression are represented by a noise term $\xi(t)$ (see Supplementary Information for a more detailed analysis).

The dynamical behaviour of equations (1) and (2) without noise can be analysed graphically by plotting their nullclines and vector field in the ComK–ComS phase space (Fig. 4a) for appropriate parameters (given in the Supplementary Information). This analysis reveals three fixed points: a stable node at low ComK (the vegetative state) and two unstable fixed points. Of these, the one at intermediate ComK is an unstable saddle and the one at high ComK (the competent state) is an unstable spiral. No limit-cycle behaviour coexists with the stable vegetative state in this parameter region (see Supplementary Information). Under these conditions, the system is capable of excitable behaviour: relatively small perturbations from the vegetative state may cause long excursions through phase space around the unstable spiral at high ComK (that is, through the competence region), as determined by the vector field. The vegetative state can be perturbed by noise in the expression of either ComK or ComS, leading to these transient differentiation events. Samples of such trajectories, generated by numerical integration of the model, are superimposed as pink lines in Fig. 4a and plotted against time in Fig. 4b.

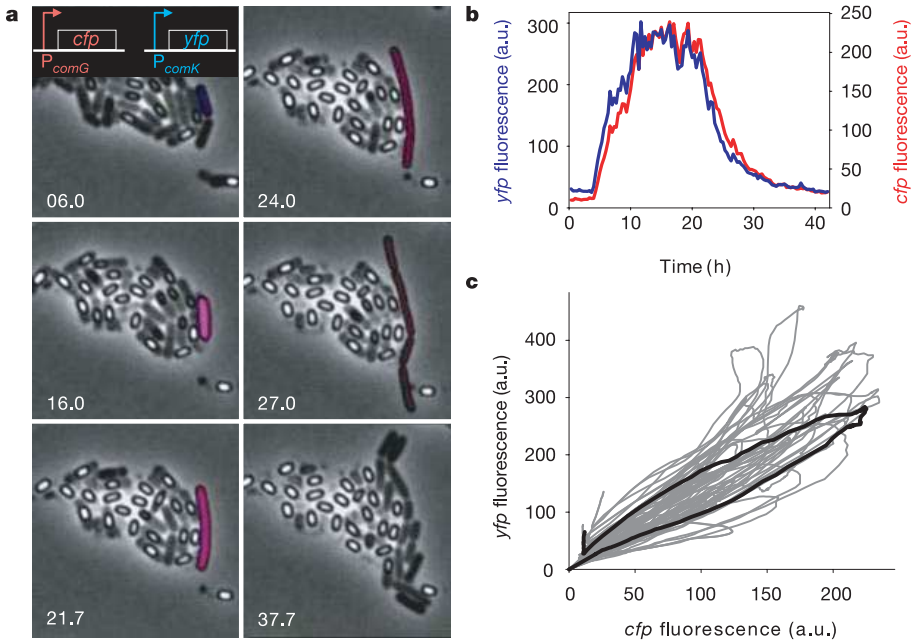


**Figure 2 | Activities of $P_{comK}$ and $P_{comG}$ promoters are highly correlated during competence.** **a**, Frames from film footage of a typical competence event. *yfp* expressed from $P_{comK}$ and *cfp* expressed from $P_{comG}$ are coloured blue and red, respectively (see also Supplementary Movie 1). Overlapping dynamics of $P_{comK}$ and $P_{comG}$ result in the purple (red plus blue) colour of the competent cell. Time (in hours) is indicated for each frame. **b**, Quantitative time series of $P_{comK}$–*yfp* (blue line) and $P_{comG}$–*cfp* (red line) obtained through semi-automated data processing of the competence event shown in **a**. $P_{comK}$ and $P_{comG}$ activities exhibit nearly identical dynamics. a.u., arbitrary units. **c**, Plot of $P_{comK}$–*yfp* versus $P_{comG}$–*cfp* obtained from all ($n = 37$) competence events in this strain. The traces are smoothed for visual clarification. Note the positive correlation between $P_{comK}$–*yfp* and $P_{comG}$–*cfp*. Highlighted in black is the competence time trace depicted in **b**.

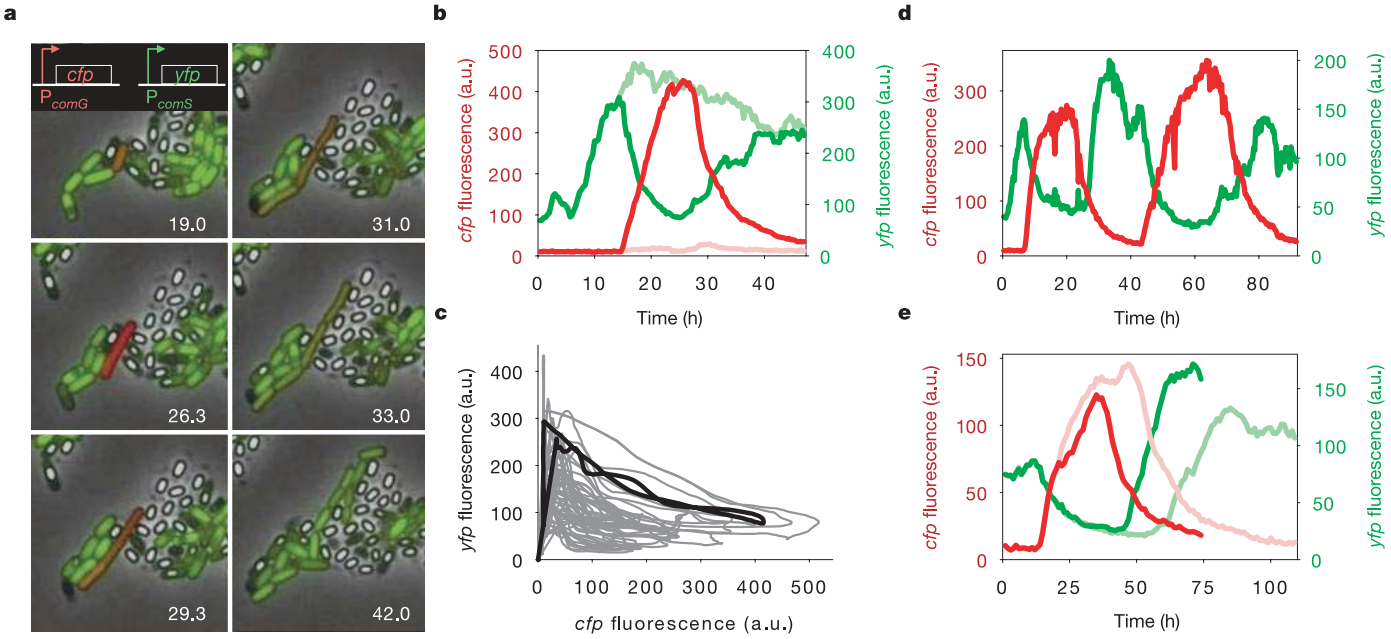


**Figure 3 | Promoter activities of $P_{comS}$ and $P_{comG}$ are anti-correlated during competence.** **a**, Frames from film footage of a typical competence event with $P_{comS}$–*yfp* and $P_{comG}$–*cfp* expression shown in green and red, respectively (see inset) (see also Supplementary Movie 2). Time (in hours) is indicated for each frame. **b**, Quantitative time series of $P_{comS}$–*yfp* (green line) and $P_{comG}$–*cfp* (red lines) for the competence event shown in **a**. Depicted in faint green and faint red are $P_{comS}$ and $P_{comG}$ activities obtained from the non-competent sister cell. Note that the negative correlation between $P_{comS}$ and $P_{comG}$ expression dynamics is only observed in the competent cell. **c**, Plot of $P_{comS}$–*yfp* versus $P_{comG}$–*cfp* obtained from all ($n = 31$) competence events in this strain. The traces are smoothed for visual clarification. Note the negative correlation between $P_{comS}$–*yfp* and $P_{comG}$–*cfp*. Highlighted in black is the competence time trace depicted in **b**. **d**, Quantitative time traces of consecutive competence events within a single cell lineage. The colour scheme is identical to that described for **b**. **e**, Quantitative time traces of $P_{comS}$–*yfp* and $P_{comG}$–*cfp* measured in sister cells that both undergo competence. The colour scheme is identical to that described for **b**. Note the different durations of competence in sister cells (see Supplementary Fig. S7).

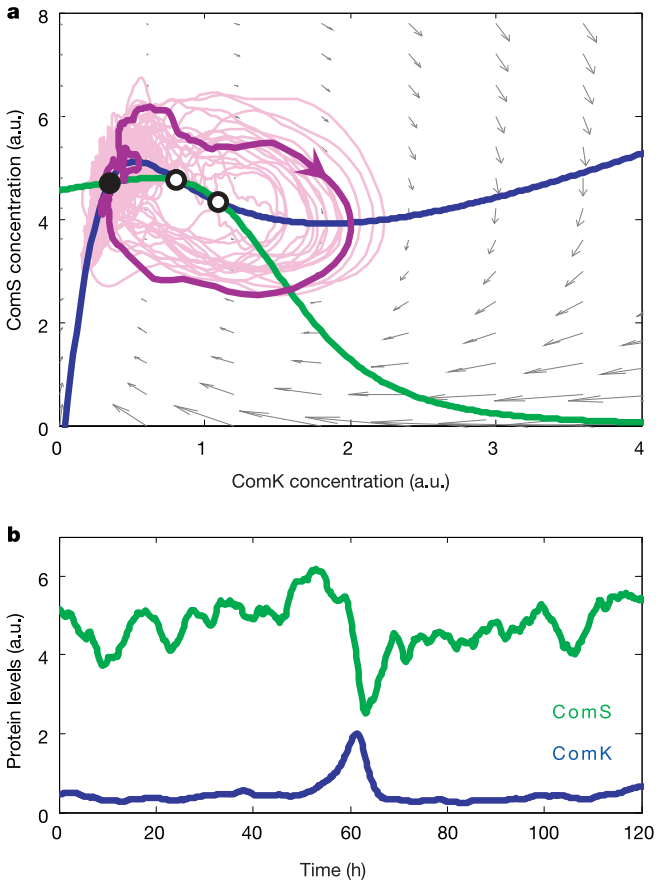


**Figure 4 | Modelling of the core competence network reveals an excitable system. a**, Phase plane diagram formed by the system of equations shown in Box 1. Nullclines for equations (1) and (2) are shown in blue and green, respectively. Grey arrows represent the vector field of the dynamical system. The stable steady-state corresponding to vegetative growth is indicated with a black filled circle. The saddle and the unstable competent fixed points are indicated with open circles. A set of excursion trajectories is shown in pink, with a single representative trajectory of the system highlighted in purple. Initiation of excursions in phase space is triggered by noise (Box 1), and trajectories are determined by the phase space vector field. **b**, Simulations of ComS (green) and ComK (blue) activities as a function of time. Note the negative correlation between the ComS and ComK levels during competence, consistent with experimental observations.

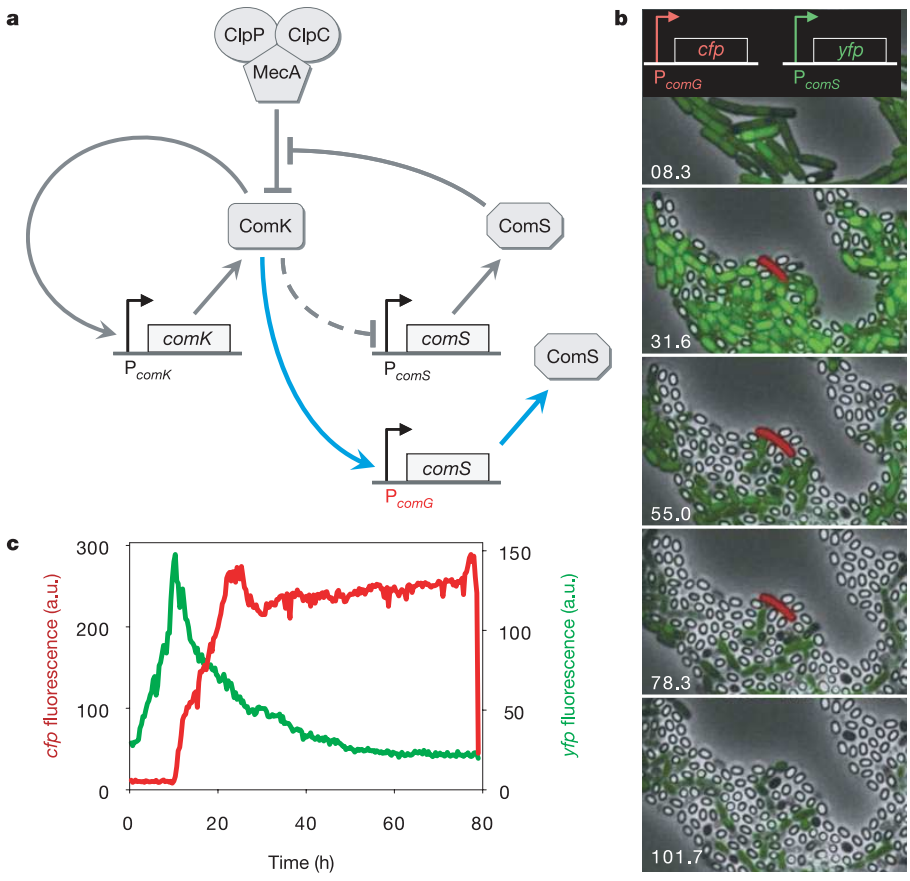


**Figure 5 | Competence lock through feedback bypass. a**, Network schematic depicting in blue the extra link introduced to bypass the native ComS-mediated negative feedback loop (FeBy strain). Note that the native network is left intact (see Fig. 1a). **b**, Frames from film footage of a typical competence event in the FeBy strain, with $P_{comS}$ and $P_{comG}$ activities depicted in green and red, respectively (see also Supplementary Movie 3). **c**, Quantitative time series of $P_{comS}$–*yfp* (green line) and $P_{comG}$–*cfp* (red line) for the event shown in **b**. The FeBy cell enters competence, but cannot exit from competence and eventually lyses (note the sudden drop after nearly 80 h).

To understand how the network structure supports the dynamics of competence, we built a differential equation model of the MeKS module that incorporates noise. In this model, two feedback loops regulate ComK: the positive loop is based on direct transcriptional auto-activation; the negative loop is indirect and involves ComS-modulated degradation of ComK (Fig. 1a, Box 1 and Supplementary Information). This model contains a regime in which noise in the production of either ComK or ComS can trigger large excursions in phase space that resemble experimental observations (Fig. 4). Thus, this model of excitability accounts in a natural way for the dynamics of competence observed in experiments.

How does the circuit generate transient competence events? This behaviour is caused by the combination of a fast positive and slow negative feedback. Positive feedback motifs are well known generators of bistability in cell biology[22,23]. Combinations of positive and negative feedbacks are crucial elements of dynamic processes in biology such as the cell cycle[24]. In the present system, noise can induce escape from the otherwise stable vegetative state and turn the system 'on' via the ComK positive feedback, as suggested previously by other groups[11,12]. On a slower timescale, this initiates the ComS-mediated negative feedback. Reduction in ComS levels eventually shuts the system back 'off' through an increase in ComK degradation, returning the cell to its vegetative state. In this way, ComS has a dual role in the system: on the one hand it is necessary to initiate competence, by blocking degradation of ComK and allowing positive autoregulation to take effect; on the other hand, repression of ComS is necessary for exit from competence, because reduction in ComS levels favours ComK degradation by MecA.

The excitable model of competence induction makes a strong prediction: interfering with the ComS-mediated negative feedback loop should stabilize the competent state without changing the frequency with which cells become competent (Supplementary Fig. S6). To test this prediction, we constructed a feedback bypass (FeBy) strain of *B. subtilis* containing a single chromosomal copy of $P_{comG}$ driving the expression of *comS* (Fig. 5a). This modification leaves the native competence network intact: the added *comS* gene is expressed only in competent cells. By expressing additional ComS in this way, the natural negative feedback is rendered ineffective.

We performed time-lapse microscopy on the FeBy strain (Fig. 5b and Supplementary Movie 3). The resulting movies show that FeBy cells become competent at normal frequencies ($4.2 \pm 0.8\%$; $n = 32$ out of 754), but most of these competent cells fail to return to vegetative growth. In a wild-type culture, 61% of cells successfully exit competence ($n = 136$), compared to only 12% of FeBy cells ($n = 55$). $P_{comG}$ expression levels in competent FeBy cells do not significantly exceed those in wild-type cells, suggesting that the defect in exit is not simply due to overexpression of ComK. As in wild-type cells, a negative correlation between $P_{comG}$ and $P_{comS}$ is observed in FeBy cells (Fig. 5c). Thus, the FeBy cells behave similarly to wild-type cells during entry into competence, and differ specifically in their reduced ability to exit.

Even in well-characterized cellular networks, it is generally difficult to connect circuit structure to circuit dynamics[25]. Within the complex *B. subtilis* competence circuitry however, the relatively simple MeKS module can explain the transient and probabilistic features of competence dynamics. This suggests that during competence not all of the known interactions within the larger competence circuit are important all of the time.

In the FeBy strain, a single rewiring step transformed a transient differentiation process into a terminal one. This reflects a degree of plasticity in the excitable circuit module. Notably, the architecture of this circuit is similar to the circadian clock and cell cycle oscillators, which also contain combined positive–negative feedback loops[24,26,27]. Excitability is found in biological systems that process information such as neurons, where the frequency of events, but not their shape or amplitude, needs to be tuned[28]. Our results show that excitability also operates in an intracellular genetic network controlling transient differentiation—an event on a very different timescale that uses completely different molecular components. Evidently, analogous functional roles for excitable dynamics exist in microbial and neuronal systems. We anticipate that this circuit design may therefore represent a general solution to a range of biological design problems.

## METHODS

For detailed information on all methods, see Supplementary Information

**Strain construction.** Promoter–*yfp*/*cfp* fusions were generated using fusion polymerase chain reaction techniques and cloned into *B. subtilis* integration vectors pDL30 (gift from J. Dworkin), pPyr-Cm and pSac-Cm (constructed by R. Middleton). The strain background was *B. subtilis* strain PY79.

**Preparation of cells for microscopy.** Cells were grown at 37 °C in Luria broth to an optical density of 1.8 and re-suspended in 0.5 volume of resuspension medium (RM) supplemented with 0.02% glucose. After 1.5 h incubation at 37 °C, cells were applied onto a 1.5% agarose pad made with RM and placed into a coverslip-bottom Willco dish for imaging.

**Time-lapse microscopy.** Growth of microcolonies was observed with fluorescence time-lapse microscopy at 37 °C using an Olympus IX-81 inverted microscope with a motorized stage (ASI). Image sets were acquired every 20 min with a Hamamatsu ORCA-ER camera. Custom Visual Basic software was used to automate image acquisition and microscope control.

**Data analysis.** Time-lapse microscopy data were analysed with custom software written in Matlab.

**Model analysis.** Mathematical models were simulated using custom-made software and further analysed using the analytic continuation software packages AUTO and DDE-BIFTOOL.

**Received 15 September 2005; accepted 18 January 2006.**


1. Dupin, E., Real, C., Glavieux-Pardanaud, C., Vaigot, P. & Le Douarin, N. M. Reversal of developmental restrictions in neural crest lineages: transition from Schwann cells to glial-melanocytic precursors *in vitro*. *Proc. Natl Acad. Sci. USA* **100,** 5229–5233 (2003).
2. Lee, E. J., Russell, T., Hurley, L. & Jameson, J. L. Pituitary transcription factor-1 induces transient differentiation of adult hepatic stem cells into prolactin-producing cells *in vivo*. *Mol. Endocrinol.* **19,** 964–971 (2005).
3. Meeks, J. C., Campbell, E. L., Summers, M. L. & Wong, F. C. Cellular differentiation in the cyanobacterium *Nostoc punctiforme*. *Arch. Microbiol.* **178,** 395–403 (2002).
4. Grossman, A. D. Genetic networks controlling the initiation of sporulation and the development of genetic competence in *Bacillus subtilis*. *Annu. Rev. Genet.* **29,** 477–508 (1995).
5. Hamoen, L. W., Venema, G. & Kuipers, O. P. Controlling competence in *Bacillus subtilis*: shared use of regulators. *Microbiology* **149,** 9–17 (2003).
6. Lindner, B., Garcia-Ojalvo, J., Neiman, A. & Schimansky-Geier, L. Effects of noise in excitable systems. *Phys. Rep.* **392,** 321–424 (2004).
7. Hahn, J., Kong, L. & Dubnau, D. The regulation of competence transcription factor synthesis constitutes a critical control point in the regulation of competence in *Bacillus subtilis*. *J. Bacteriol.* **176,** 5753–5761 (1994).
8. Hahn, J., Luttinger, A. & Dubnau, D. Regulatory inputs for the synthesis of ComK, the competence transcription factor of *Bacillus subtilis*. *Mol. Microbiol.* **21,** 763–775 (1996).
9. van Sinderen, D. *et al. comK* encodes the competence transcription factor, the key regulatory protein for competence development in *Bacillus subtilis*. *Mol. Microbiol.* **15,** 455–462 (1995).
10. van Sinderen, D. & Venema, G. *comK* acts as an autoregulatory control switch in the signal transduction route to competence in *Bacillus subtilis*. *J. Bacteriol.* **176,** 5762–5770 (1994).
11. Maamar, H. & Dubnau, D. Bistability in the *Bacillus subtilis* K-state (competence) system requires a positive feedback loop. *Mol. Microbiol.* **56,** 615–624 (2005).
12. Smits, W. K. *et al.* Stripping *Bacillus*: ComK auto-stimulation is responsible for the bistable response in competence development. *Mol. Microbiol.* **56,** 604–614 (2005).
13. Turgay, K., Hahn, J., Burghoorn, J. & Dubnau, D. Competence in *Bacillus subtilis* is controlled by regulated proteolysis of a transcription factor. *EMBO J.* **17,** 6730–6738 (1998).
14. Ogura, M., Liu, L., Lacelle, M., Nakano, M. M. & Zuber, P. Mutational analysis of ComS: evidence for the interaction of ComS and MecA in the regulation of competence development in *Bacillus subtilis*. *Mol. Microbiol.* **32,** 799–812 (1999).
15. Rosenfeld, N., Young, J. W., Alon, U., Swain, P. S. & Elowitz, M. B. Gene regulation at the single-cell level. *Science* **307,** 1962–1965 (2005).
16. Ozbudak, E. M., Thattai, M., Kurtser, I., Grossman, A. D. & van Oudenaarden, A. Regulation of noise in the expression of a single gene. *Nature Genet.* **31,** 69–73 (2002).
17. Elowitz, M. B., Levine, A. J., Siggia, E. D. & Swain, P. S. Stochastic gene expression in a single cell. *Science* **297,** 1183–1186 (2002).

18. Haijema, B. J., Hahn, J., Haynes, J. & Dubnau, D. A. ComGA-dependent checkpoint limits growth during the escape from competence. *Mol. Microbiol.* **40,** 52–64 (2001).
19. Serror, P. & Sonenshein, A. L. CodY is required for nutritional repression of *Bacillus subtilis* genetic competence. *J. Bacteriol.* **178,** 5910–5915 (1996).
20. Nakano, M. M. & Zuber, P. The primary role of *comA* in establishment of the competent state in *Bacillus subtilis* is to activate expression of *srfA*. *J. Bacteriol.* **173,** 7269–7274 (1991).
21. Hahn, J. & Dubnau, D. Growth stage signal transduction and the requirements for *srfA* induction in development of competence. *J. Bacteriol.* **173,** 7275–7282 (1991).
22. Isaacs, F. J., Hasty, J., Cantor, C. R. & Collins, J. J. Prediction and measurement of an autoregulatory genetic module. *Proc. Natl Acad. Sci. USA* **100,** 7714–7719 (2003).
23. Xiong, W. & Ferrell, J. E. Jr. A positive-feedback-based bistable 'memory module' that governs a cell fate decision. *Nature* **426,** 460–465 (2003).
24. Pomerening, J. R., Kim, S. Y. & Ferrell, J. E. Jr. Systems-level dissection of the cell-cycle oscillator: bypassing positive feedback produces damped oscillations. *Cell* **122,** 565–578 (2005).
25. Lahav, G. *et al.* Dynamics of the p53-Mdm2 feedback loop in individual cells. *Nature Genet.* **36,** 147–150 (2004).
26. Hardin, P. E. The circadian timekeeping system of *Drosophila*. *Curr. Biol.* **15,** R714–R722 (2005).
27. Vilar, J. M., Kueh, H. Y., Barkai, N. & Leibler, S. Mechanisms of noise-resistance in genetic oscillators. *Proc. Natl Acad. Sci. USA* **99,** 5988–5992 (2002).
28. Keener, J. & Sneyd, J. *Mathematical Physiology* (Springer, New York, 1998).

**Supplementary Information** is linked to the online version of the paper at www.nature.com/nature.

**Acknowledgements** We thank U. Alon, D. Dubnau, J. Dworkin, A. Eldar, J. Ferrell, R. Kishony, B. Lazazzera, R. Losick, A. Raj, B. Shraiman, D. Sprinzak, M. Surette and members of the laboratory for comments. G.M.S. is supported by the Caltech Center for Biological Circuit Design. J.G.-O. acknowledges financial support from the Generalitat de Catalunya and the Ministerio de Educacion y Ciencia (Spain). M.B.E. acknowledges support from the Searle Scholars Program and the Burroughs Wellcome Fund CASI program.

**Author Information** Reprints and permissions information is available at npg.nature.com/reprintsandpermissions. The authors declare no competing financial interests. Correspondence and requests for materials should be addressed to M.B.E. (melowitz@caltech.edu).